

Mechanical Design and Analysis of LHC Inner Triplet Quadrupole Magnets at Fermilab

N. Andreev, T. Arkan, R. Bossert, D. R. Chichili, S. Feher, J. Kerby, M. J. Lamm, A. Makarov, A. Nobrega, I. Novitski, D. Orris, J. P. Ozelis, M. Tartaglia, J. C. Tompkins, S. Yadav, A. V. Zlobin

Fermi National Accelerator Laboratory, Batavia, IL., USA

Abstract-- A series of model magnets is being constructed and tested at Fermilab in order to verify the design of high gradient quadrupole magnets for the LHC interaction region inner triplets. The 2m models are being built in order to refine the mechanical and magnetic design, optimize fabrication and assembly tooling, and ensure adequate quench performance. This has been carried out using a complementary combination of analytical and FEA modeling, empirical tests on 0.4m mechanical assemblies, and testing of model magnets during fabrication and under cryogenic conditions. The results of these tests and studies have led to improvements in the design of the magnet end restraints, to a preferred choice in coil end part material, and to a better understanding of factors affecting coil stress throughout the fabrication and operational stages.

I. INTRODUCTION & DESIGN APPROACH

Fermilab, in collaboration with Lawrence Berkeley National Laboratory, is developing a high gradient quadrupole for use as part of the LHC interaction region triplets. A series of short model magnets is being produced to optimize design and fabrication details and to ensure adequate performance, which is strongly determined by the mechanical design.

Optimization of the magnet mechanical design is being pursued through comparison of results obtained from analytical calculations, finite-element method models, short mechanical assemblies, and fully instrumented model magnets. The short (~40cm) mechanical assemblies are instrumented with capacitance strain gauges and consist only of the magnet coils' straight sections and collar structure. They are used to empirically confirm the relationship between coil size, modulus, and azimuthal pre-stress.

Finally, short (1.9m) fully instrumented model magnets (HGQ) are fabricated utilizing the latest design and materials choices and then tested at the Fermilab Vertical Magnet Test Facility (VMTF)[1], where their mechanical, quench, and magnetic performance is extensively studied. Recent results of quench and magnetic testing are reported elsewhere [2][3][4].

II. DESIGN DESCRIPTION

A. General Overview

The mechanical design of the Fermilab HGQ magnet consists of a 2-layer $\cos(2\theta)$ coil structure supported by stainless steel collars, which are surrounded by a cold iron yoke and stainless steel skin capped with steel end plates, as shown in Fig. 1. Coil azimuthal and radial support is provided

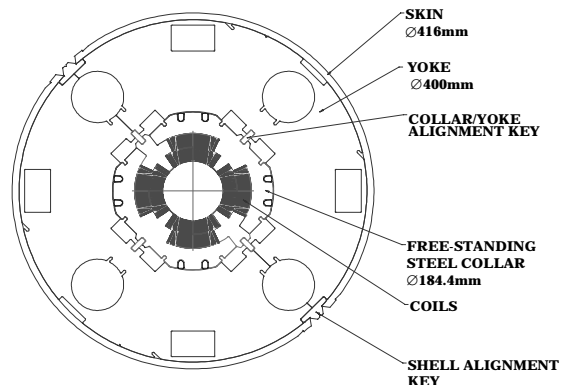


Fig. 1. Cross section of the HGQ magnet design.

by the collars. The iron yoke is magnetically aligned to the coils but does not provide any additional support. Longitudinal support and restraint of the coils is provided by end loading screws (bullets) which apply an axial load to the coils that is reacted via the end plates by the stainless steel outer shell.

B. Collared Coil

The coils are wound using Rutherford-type NbTi cable, insulated with Kapton® film with a polyimide adhesive. The end spacers of the coils were fabricated using G-10, Ultem®, and G-11, with G-11 the latest and preferred choice. The coils are cured under pressure to a fixed size at elevated temperatures.

The coils are supported in the body by 1.5mm thick Nitronic 40 stainless steel collars (welded into 75mm long packs) symmetrically applied under pressure and locked in place using tapered stainless steel keys. The collar laminations in a pack alternate between full collars and 'pole-only' inserts, so that they can be assembled as opposing pairs, 90 degrees apart, onto the coil package, yet provide uninterrupted azimuthal support of the coils. Before the collars are installed inner to outer coil splicing is performed, quench protection heaters are inserted, and ground insulation applied.

C. Yoke and Skin

The collared coil assembly is surrounded by a laminated two-piece iron yoke that is aligned to the coils using bronze keys. The iron yoke provides magnetic field tuning and flux return, and acts as a spacer for the outer shell. The iron yoke is constrained by an 8mm thick stainless steel shell that is aligned to the yoke using full-length stainless steel keys, which also provide the optimal geometry for the shell weld

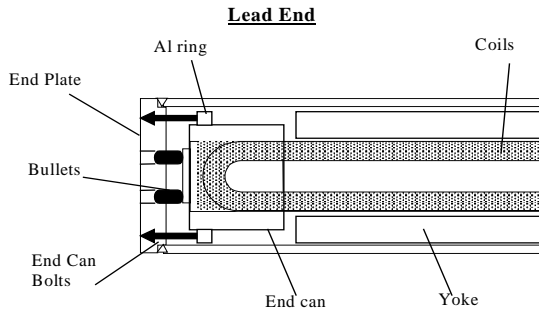


Fig. 2. Schematic of end can and restraint method used in magnets HGQ05 and later.

joint. The two halves of the skin are welded simultaneously from both sides, using multiple passes.

D. End Support and Restraint

Radial support and azimuthal compression of the coil ends is provided by an aluminum end can and G-11 collets. The profiles of the end can and collets are tapered so that as they are installed longitudinally, they provide radial compression and support. Longitudinal support of the coils is provided by 50mm thick stainless steel end plates that are welded to the outer shell, as shown in Fig. 2. Loading screws (bullets) mounted into the end plates apply longitudinal load to the coils. The end cans are bolted to the end plates in an effort to minimize coil displacement away from the end plates during cooldown. Longitudinal expansion towards the end plates during excitation is reacted only by the bullets.

III. ANALYSIS AND OPTIMIZATION

In order to verify that the chosen design would satisfy the mechanical requirements, a complementary program of FEM analysis, empirical studies, and full-scale magnet tests was employed. The primary areas of concern were :

- i.) optimizing coil size and modulus
- ii.) providing proper coil azimuthal stress
- iii.) maintaining longitudinal coil support
- iv.) controlling cold mass twist

Coil size and modulus optimization is itself a significant effort with pronounced bearing on magnet mechanical and magnetic performance, and is described in its entirety elsewhere [5].

A. Coil Azimuthal Stress

The collar design for the HGQ magnet was optimized using a 2-D ANSYS® model, utilizing the measured coil properties and octant symmetry. The model includes the inner and outer coils, insulation, bearing strips, and stainless steel collars. The collar pack is modeled as three separate pieces: a front collar, a pole insert, and a back collar. The pole insert and back collar are joined together in the model by two spot welds, while three are used in the actual assembly. Constraint equations on the collar mid-planes enforce rotational symmetry, with additional constraints for the collars provided

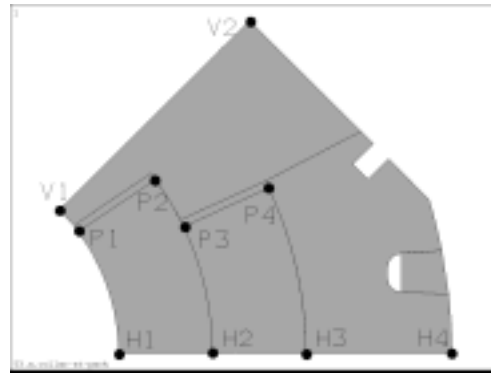


Fig. 3. Computational model of the HGQ collar and coils indicating nodes where displacements from the nominal geometry due to coil stress are calculated and used for comparison with measured values.

by the keys. Material interfaces are presented with one-dimensional gaps oriented perpendicular to the interface without frictional effects.

TABLE I.
RESULTS OF MECHANICAL MODEL AZIMUTHAL COIL STRESS STUDIES

	Mechanical Model	#6	#6A	#6B	#6C
Target (shimmed) coil size (μm)	inner	200	75	150	150
	outer	150	75	125	125
Coil stress from FEA model (MPa)	inner	74	23	53	53
	outer	57	37	51	51
Measured coil stress (MPa)	inner	86	43	57	54
	outer	70	54	60	60

The model presented in Fig. 3 shows the material components of the model and the points where their displacements are calculated. Additionally, the pressure distributions along segments defined by these points are calculated.

To refine these results, several mechanical models were built. By direct measurement of coil stress using strain gauges and indirectly through collar outer diameter measurements, the relationship between coil size, modulus, and pre-stress can be verified and improved. Additionally, the optimal coil size to yield the required coil stress can be calculated. Table I lists the results from one series of mechanical model investigations used to optimize the HGQ magnet coil shim scheme.

B. Longitudinal Coil Support & End Restraint

Measurement of the azimuthal size and modulus of the coil ends indicated significant non-uniformity due to the influence of the end part material and geometry of the current blocks. This can lead to non-uniform and, in some cases, insufficient coil pre-stress. Since it is desirable to match the coil stress in the ends to that in the straight section, an ANSYS® model of the ends was used to calculate the radial deflection of the aluminum end cans expected when the coil stress there met this condition. Measurements of the stressed and un-stressed end can diameter and tests with pressure sensitive film (Fuji film) confirmed the model predictions. From this the appropriate amount shim needed in the end

regions of the coils was determined. Based on these studies an end can radial deflection of 125-150 μm is expected.

This ANSYS® model also was used to determine the change in coil end stress resulting from thermal contraction at cryogenic temperatures. Along with observed magnet performance [6], this indicated that the end part material used in previous model magnets had undesirable modulus of elasticity and thermal contraction characteristics, leading to an substantial loss of coil pre-stress upon cooldown, requiring excessive amounts of shim to correct. This was addressed by utilizing G-11 as the end part material.

C. Cold Mass Twist

The first few HGQ model magnets showed excessive twist of the cold mass, on the order of 1.0 mrad/m, significantly higher than the 0.2 mrad/m believed to be acceptable in production magnets. This was thought to be due to non-uniform welding of the shell, since inspection of the contact tooling flatness revealed no defects, and the twist was consistently in the same direction. Welding experiments confirmed that one of the welding torches moved faster than the other, leading to an asymmetry in weld progress. This was mitigated by offsetting the slower welding torch. A mechanical model and magnet HGQ07 were welded with this offset, reducing the twist to 0.18 mrad/meter.

IV. MEASURED PERFORMANCE

A. Warm Measurement

Magnet mechanical performance during and after assembly can be characterized by coil size, coil modulus, collared coil stress, collared coil outside diameter (O.D.), end can radial deflection, and longitudinal coil force.

Coil azimuthal size and modulus are determined by compressing the cured coils and measuring them at various pressures in comparison with a standard steel block. This information, in conjunction with results of ANSYS® calculations, mechanical model, and previous magnet experience, is used to determine the proper shim size required to provide adequate coil stress in the assembled magnet.

Coil stress measurements are performed during the collaring process to verify that the correct coil pre-stress is being achieved. If this is not the case, the collared coils are disassembled and shimming is added to or removed from the coil pole faces. Coil stress measurements are also performed before and after yoking.

Similarly, measurements of the collared coil assembly outer diameter are used to determine average coil pre-stress by comparing measurements with predictions from ANSYS®, analytical, and mechanical model results. These measurements also indicate the uniformity of coil stress. In general this measurement is not a sensitive indicator of coil stress, as longitudinal coupling between collars and radial coupling between coils obscures detailed behavior.

Coil stress in the ends is inferred from measurements taken of the outer diameter of the aluminum cans that surround and constrain the coil ends. Shim is added or

removed from the collets' inner surface until the target end can deflection is obtained.

Longitudinal support of the coils is directly measured using strain gauge-based force transducers. End loading is increased until the target end force is observed. This target end force is determined by ensuring that some non-zero end load remains when the magnet is at cryogenic temperatures.

TABLE II
HGQ COIL AZIMUTHAL STRESS AND LONGITUDINAL LOAD SUMMARY

		HGQ05	HGQ06	HGQ07
Measured Coil Stress	(inner) (MPa)	77	66	68
	(outer) (MPa)	63	68	74
Calculated Coil Stress (FEA)	(inner) (MPa)	78	59	65
	(outer) (MPa)	50	65	72
Coil Longitudinal	(lead end) (kN)	10.5	9.4	2.2
Pre-Load	(non-lead end) (kN)	10.2	9.4	0.0

Mechanical measurements are presented in Table II for the latest series of short HGQ model magnets, generally indicating good agreement between measured and expected values. In magnet HGQ07 the end loading screws (bullets) were left completely loose at the non-lead end and only minimally tightened at the lead end, in order to investigate the effects of end loading on quench performance. Nominal end load is to be applied for a subsequent test cycle.

B. Cryogenic Testing

The short model magnets are tested in the Fermilab VMTF where coil stress, end load, and cold mass shell stress measurements are performed. Measurements are also performed at cryogenic temperatures before excitation, in order to determine the effects of thermal contraction on coil stress and longitudinal load. Table III summarizes the cryogenic mechanical performance of the latest HGQ model magnets. In general there is good agreement between expected and observed behavior (the apparent gain in coil stress upon cooldown for magnet HGQ06 is believed to be an artifact of beam gauge yielding [7]).

A typical example of outer coil azimuthal stress as a function of excitation current for magnets HGQ05 and 07 is given in Fig. 4. (Due to yielding effects with inner coil strain gauges in earlier HGQ magnets, they were omitted from this latest series [7].) In this figure we see the essentially linear decrease of coil stress with $(I_{\text{mag}})^2$, in excellent agreement with expectations. To date, coil unloading has not been observed in any of the model magnets.

Longitudinal load on the coil is likewise measured during magnet excitation and before quench testing (in order to measure the loss of longitudinal pre-load due to coil shrinkage). The longitudinal coil force as a function of excitation current squared for magnets HGQ05 and HGQ06 is given in Fig. 5, which shows that positive contact between the ends of the coils and the loading screws was maintained upon cooldown, ensuring adequate support of the coils during excitation. In previous model magnets end restraint was not always maintained after cooldown due to thermal contraction of the coils, or was maintained by requiring excessive longitudinal preload at 300K[8]. Use of the aluminum end

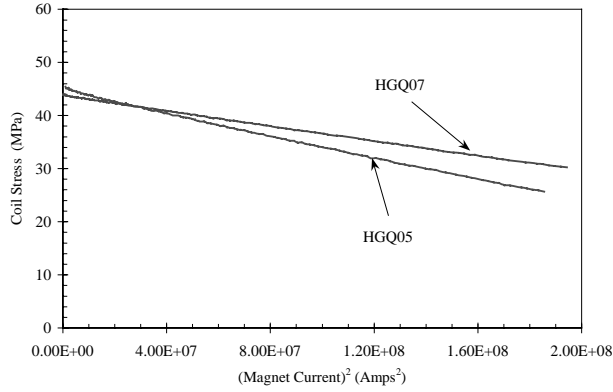


Fig. 4. Average outer coil azimuthal stress for magnets HGQ05-07 during runs to quench at 1.9K

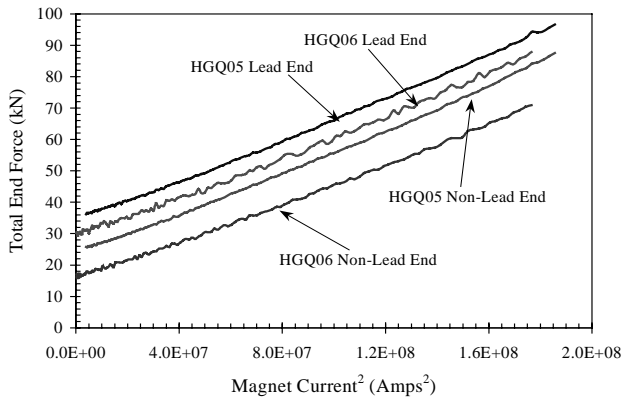


Fig. 5. Total coil end loads for magnets HGQ05 & HGQ06 during a run to quench at 1.9K

cans and G-10/G-11 end part materials has alleviated this problem in the latest series of models.

TABLE III
MODEL MAGNET MECHANICAL CRYOGENIC PERFORMANCE

	HGQ05	HGQ06	HGQ07
Azimuthal Stress Change (outer) (MPa) (300K - 1.9K)	-6	--	-29
Azimuthal Lorentz Force (inner) (MPa/kA ²)	0.24	0.41	0.16
(outer) (MPa/kA ²)	0.13	0.08	0.07
Long. Force Change (lead end) (kN) (300k-1.9K)	-5.4	-4.7	-1.6
(non-lead end) (kN)	-6.1	-6.4	--
Longitudinal Lorentz (lead end) (kN/kA ²)	.089	.088	.071
Force (non-lead end) (kN/kA ²)	.091	.083	--

Relative longitudinal strain is also measured as a function of length along the cold mass during excitation. In general, the measured strains at the magnet ends match that expected from the measured coil end forces transferred to the end plate. The longitudinal strain sensitivity along the cold mass is shown in Figure 6 for magnets HGQ05-07. Magnet HGQ07 was only instrumented along half of its length (from non-lead end to center), but in two different azimuthal positions (0 and 45 degrees with respect to the quadrant 1 axis). Since the non-lead end loading screws were not tightened for magnet

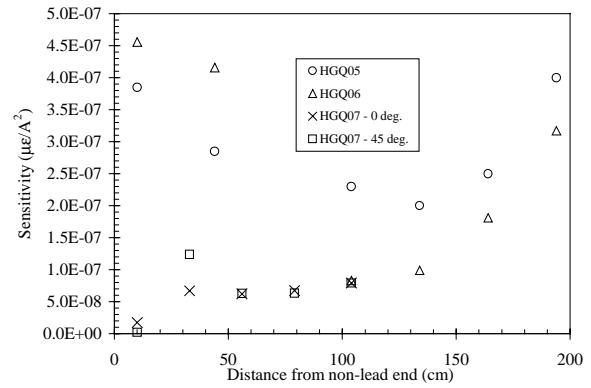


Fig. 6. Longitudinal shell strain sensitivity along the cold mass length

HGQ07, no load was applied to the non-lead end plate. This is confirmed by the zero strain sensitivity measured at the end plates. The non-uniform distribution of strain sensitivity along the cold mass length is not presently understood, since it is expected that coil longitudinal load should only be transferred to the skin via the end plates, and not through collar/yoke/shell interactions.

V. CONCLUSIONS

The HGQ mechanical design has been refined and improved through a combination of analytical, computational, and empirical studies. Quench performance has improved substantially, and is well reproduced among magnet assemblies. The essential design details leading to achievement of the performance goals are being finalized. Two additional model magnets will be fabricated in order to refine production techniques and test minor modifications to cable design, in preparation for full-scale prototype fabrication.

ACKNOWLEDGMENTS

The authors gratefully acknowledge the efforts of the staffs of the Fermilab Technical Division's Development & Test and Engineering & Fabrication departments.

REFERENCES

- [1] M.J. Lamm et al., "A new facility to test superconducting accelerator magnets", PAC '97, Vancouver, Canada, 1997.
- [2] N. Andreev et al., "Quench behavior of quadrupole model magnets for the LHC inner triplets at Fermilab", submitted to MT16, 1999.
- [3] N. Andreev et al., "Quench protection studies of LHC interaction region quadrupoles at Fermilab", submitted to MT16, 1999.
- [4] N. Andreev et al., "Field quality of model quadrupole magnets for the LHC interaction regions at Fermilab", submitted to MT16, 1999.
- [5] N. Andreev et al., "Study of Kapton insulated superconducting coils manufactured for the LHC inner triplet model magnets at Fermilab", submitted to MT16, 1999.
- [6] J. Kerby et al., "Design, development and test of 2m model magnets for the LHC inner triplet", IEEE Trans. Appl. Supercond. v.9, pp. 689-692, June 1999.
- [7] S. Yadav, J. Kerby, J. P. Ozelis, "Analysis of parameters affecting beam gauge performance", submitted to MT16, 1999.
- [8] R. Bossert et al., "Mechanical design and performance of the Fermilab high gradient quadrupole model magnets for the LHC interaction regions", IEEE Trans. Appl. Supercond. v.9, pp. 459-462, June 1999.